Quantum chaos: an introduction via chains of interacting spins-1/2

Aviva Gubin and Lea F. Santos
Department of Physics, Yeshiva University, 245 Lexington Ave, New York, NY 10016, USA

This work introduces aspects of quantum chaos by focusing on spectral statistical properties and structures of eigenstates of quantum many-body systems. Quantum systems whose classical counterparts are chaotic have properties that differ from those of quantum systems whose classical counterparts are regular. One of the main signatures of what became known as quantum chaos is a spectrum showing repulsion of the energy levels. Here, we show how level repulsion may develop in one-dimensional systems of interacting spins-1/2 which are devoid of random elements and involve only two-body interactions. Chains of interacting spins-1/2 are prototype quantum many-body systems. They are used to study subjects as diverse as quantum computing, quantum phase transition, quantum transport, and quantum control. Nonetheless, they are simple enough to be accessible to students. In addition to the statistics of eigenvalues, we analyze also how the structure of the eigenstates may indicate chaos. We make available online all computer codes used to obtain the data for the figures. This should allow students and professors to easily reproduce our results and to further explore new questions.

I. INTRODUCTION

Classical chaos is related to the extreme sensitivity of the dynamics of a system to its initial conditions, a concept that can be traced back to Poincaré [1]. In his words, 'A small error in [the initial conditions] will produce an enormous error in the [final phenomena]. Prediction becomes impossible...'. The main features of classically chaotic systems can be well illustrated with dynamical billiards. A dynamical billiard may be thought of as a billiard table with no friction where a particle reflects elastically from boundaries that can have any shape. The motion of the particle bouncing around is represented in phase space by a trajectory whose evolution is restricted to a surface of constant energy. Depending on the shape of the billiard, the system may become chaotic. This means that two trajectories with very close initial conditions will diverge exponentially in time. The rate of this separation is characterized by the so-called Lyapunov exponent [2]. The trajectories may become ergodic, as well. Ergodicity implies that after a long time the particle will have visited the entire surface of constant energy. Equivalently, we may say that after a long time, the particle is equally likely to be found in any point of the accessible phase space.

In the quantum world, the notion of phase-space trajectories loses its meaning due to Heisenberg uncertainty principle. Nevertheless, since classical physics is but a limit of quantum physics, as stated by the correspondence principle, it is natural to search for quantum signatures of classical chaos. This is the subject of what became known as quantum chaos [3–5].

Quantum chaos is a very broad subject area. Our intention here is not to review the whole subject, but to focus on a particular aspect of it, namely the studies of spectral statistics and structures of eigenstates of quantum many-body systems as they transition from the regular to the chaotic domain. However, as a preparation for our goal, we give in the next paragraphs a brief idea of some of the important topics of the field (more details may be found in the books [6–9] and in the articles cited below).

Quantum chaos encompasses, for instance, semiclassical theories aiming at establishing direct links between the trajectories of classically chaotic systems and the properties of these systems in the quantum limit. Main advances in this direction were achieved by the periodic-orbit theory. This theory provides a way to compute the spectrum of a quantum system from its classical periodic orbits (trajectories that repeat themselves after a period). An excellent first introduction to the subject was written by Gutzwiller [4], a pioneer of this line of research. Gutzwiller's method allowed for the development of a theory of 'scars' [9, 10]. Scars refer to the interesting structure of some eigenstates, which concentrate along the classical periodic orbits of chaotic systems. They were systematically studied by Heller [11] and the first experimental observations occurred in quantum billiards [3]. Quantum billiards obey the laws of quantum mechanics and correspond to minituarized versions of dynamical billiards.

Another important step towards the development of a quantum chaos theory came from the verification that the distribution of the spacings between neighboring energy levels of a quantum billiard depends on the billiard's classical counterpart [5, 12–14]. If the latter is chaotic, the energy levels are highly correlated and repel each other; if it is regular (integrable), the energy levels are uncorrelated, randomly distributed, and can cross. Level repulsion became seen as one of the main features of quantum chaos. It was observed in various other quantum systems, such as atoms in strong magnetic fields [3], systems of coupled particles [7–9, 15], and even in distributions of prime numbers [16].

In this article we focus on systems of coupled particles, more specifically quantum systems of many interacting particles, the so-called quantum many-body systems. Most of the systems studied in molecular, solid-state, and nuclear physics, involve many interacting particles. A common approach when dealing with such systems is to ignore details about the interactions and treat them statistically with random matrices. The idea behind is that when the interactions are strong and the behavior of the system sufficiently complex, generic properties should emerge. This was the path taken by Wigner in the 1950s [17], in his efforts to describe the spectrum of heavy nuclei. He employed matrices filled with random elements whose only constraint was to satisfy the symmetries of the system. The level spacing distributions of these matrices showed level repulsion and agreed surprisingly well with the data from actual nuclei spectra. Later, when level repulsion

was also verified in billiards, as mentioned above, a connection between quantum chaos and random matrices became established. Soon after the introduction of random matrices in nuclear physics, they were employed also in the analysis of the spectrum of other quantum many-body systems, such as atoms, molecules, and quantum dots [7–9, 15, 18, 19].

The application of random matrix theory is not restricted to statistics of eigenvalues, but accommodates also studies of eigenstates. Eigenstates of random matrices are random vectors, that is their amplitudes are random variables [20, 21]. All the eigenstates look similar, they spread through all basis vectors with no preferences and are therefore ergodic.

Despite the success of random matrix theory in describing spectral statistical properties, it cannot capture details about real quantum many-body systems. The fact that random matrices are completely filled with statistically independent elements implies infinite-range-interactions and the simultaneous interaction of many particles. Real systems, on the other hand, have few-body (most commonly only two-body) interactions, and are usually dominated by finite-range-interactions. A better picture of systems with finite-range-interactions is provided by banded random matrices, which were studied by Wigner himself [22]. Their off-diagonal elements are still random and statistically independent, but they are non vanishing only up to a fixed distance from the diagonal. There are also ensembles of random matrices that explicitly take into account the restriction to few body interactions, so that only the elements associated with those interactions are nonzero; an example is the Two-Body-Random-Ensemble (TBRE) [23–25] (see reviews in Refs.[21, 26]). Other models that describe systems with short-range and few-body interactions do not even include random elements, such as nuclear shell models [27] or the systems of interacting spins that we study in this article. All matrices mentioned above may still lead to quantum chaos in the sense of exhibiting level repulsion, but differences with respect to random matrices are observed. For instance, eigenstates of random matrices are completely spread (delocalized) in any basis, whereas the eigenstates of systems with few-body interactions may delocalize only in the middle of the spectrum [26–30].

Here, we study a one-dimensional system of interacting spins-1/2, where random elements are nonexistent. The system involves only two-body interactions taking place between nearest-neighbors and, in certain cases, also between next-nearest-neighbors. Depending on the strength of the couplings, the system may develop chaos. The onset of chaos is identified by computing the level spacing distribution. We also compare the level of delocalization of the eigenstates in the integrable and chaotic domains. It is significantly larger in the latter case, where the most delocalized states are found in the middle of the spectrum.

Chains of spins-1/2 are accessible systems and may be employed to expose students to a multitude of subjects. In addition to the crossover from integrability to chaos, they may be used, for example, to introduce current topics of research such as the metal-insulator transition, quantum phase transition, entanglement, spintronic and methods of quantum control. They have been considered as models for quantum computers, magnetic compounds and have recently been simulated in optical lattices [31–33].

The paper is organized as follows. Section II provides a detailed description of the Hamiltonian of a spin-1/2 chain. Section III explains how to compute the level spacing distribution and how to quantify the level of delocalization of the eigenstates. Section IV discusses how remaining symmetries of the system may hinder the signatures of chaos even when the system is chaotic. Concluding remarks are given in Sec. V.

II. SPIN-1/2 CHAIN

We study a one-dimensional spin-1/2 system (spin-1/2 chain) described by the Hamiltonian

$$H = H_z + H_{\rm NN}, \tag{1}$$

where

$$H_z = \sum_{n=1}^{L} \omega_n S_n^z = \left(\sum_{n=1}^{L} \omega S_n^z\right) + \epsilon_d S_d^z,$$
$$H_{\rm NN} = \sum_{n=1}^{L-1} \left[J_{xy}\left(S_n^x S_{n+1}^x + S_n^y S_{n+1}^y\right) + J_z S_n^z S_{n+1}^z\right] .$$

Above, $\hbar$ is set equal to 1, L is the number of sites, and $S_n^{x,y,z} = \sigma_n^{x,y,z}/2$ are the spin operators at site n, $\sigma_n^{x,y,z}$ being the Pauli matrices. The term H_z gives the Zeeman splitting of each spin n, as determined by a static magnetic field in the z direction. A spin up in the z direction is indicated as $|\uparrow\rangle$ or with the vector $\binom{1}{0}$ and a spin down $|\downarrow\rangle$ with $\binom{0}{1}$. An up-spin on site n has energy $+\omega_n/2$, while a down-spin has energy $-\omega_n/2$. A spin up corresponds then to an excitation. All sites are assumed to have the same energy splitting ω, except a single site d, whose energy splitting $\omega + \epsilon_d$ is caused by a magnetic field slightly larger than the field applied on the other sites. This site is referred to as the defect.

The second term, $H_{\rm NN}$, is known as the XXZ Hamiltonian. It describes the couplings between nearest-neighbor (NN) spins; J_{xy} is the strength of the flip-flop term $S_n^x S_{n+1}^x + S_n^y S_{n+1}^y$ and J_z the strength of the Ising interaction $S_n^z S_{n+1}^z$.

The flip-flop term exchanges the position of neighboring up and down spins according to

$$J_{xy}(S_n^x S_{n+1}^x + S_n^y S_{n+1}^y)|\uparrow_n\downarrow_{n+1}\rangle = (J_{xy}/2)|\downarrow_n\uparrow_{n+1}\rangle$$

or, equivalently, it moves the excitations through the chain. Notice that we have assumed open boundary conditions, as indicated by the sum in $H_{\rm NN}$ which goes from $n = 1$ to site $L - 1$. This means that an excitation in site 1 (or L) can only move to site 2 (or to site $L - 1$). The scenario of a ring where an excitation on site L can also move to site 1 corresponds to closed boundary conditions and is mentioned briefly in Sec. IV.

The Ising interaction implies that pairs of parallel spins have higher energy than pairs of anti-parallel spins, that is

$$J_z S_n^z S_{n+1}^z|\uparrow_n\uparrow_{n+1}\rangle = +(J_z/4)|\uparrow_n\uparrow_{n+1}\rangle, \tag{2}$$

whereas

$$J_z S_n^z S_{n+1}^z |\uparrow_n\downarrow_{n+1}\rangle = -(J_z/4)|\uparrow_n\downarrow_{n+1}\rangle. \quad (3)$$

For the chain described by H (1), the total spin in the z direction, $S^z = \sum_{n=1}^{L} S_n^z$, is conserved, *i.e.* $[H, S^z] = 0$. This is a symmetry of the system. It means that the total number of excitations is fixed; the Hamiltonian cannot create or annihilate excitations, it can only move them through the chain.

In order to write the Hamiltonian in the matrix form and then diagonalize it to find its eigenvalues and eigenstates, we need first to choose a basis. The most natural choice is the one we have used so far to describe the terms of H, which corresponds to arrays of up and down spins in the z-direction. We refer to it as the site-basis. In this basis, H_z and the Ising interaction contribute to the diagonal elements of the matrix, whereas the flip-flop term leads to the off-diagonal elements.

In the absence of the Ising interaction, the excitations move freely through the chain. In this scenario, eigenvalues and eigenstates may be analytically found. The existence of an analytical method to find the spectrum of a system guarantees its integrability. The addition of the Ising interaction may eventually lead to the onset of quantum chaos. The source of chaos is the interplay between the Ising interaction and the defect [34].

To bring the system to the chaotic regime, we set $J_{xy} = 1$ (arbitrary unit), choose $J_z = \epsilon = 0.5$ (arbitrary unit), and place the defect on site $d = \lfloor L/2 \rfloor$. This choice is based on the following factors. (i) The strength of the Ising interaction cannot be much larger than J_{xy}, because this would limit the number of effectively coupled states. Basis vectors with several pairs of parallel spins would have energy much higher than states with few pairs of parallel spins [cf. Eqs.(2), (3)] and J_{xy} would not be able to effectively couple them. As a result, the eigenstates would count with the participation of a small portion of the basis vectors and would therefore be localized. This contradicts the idea of chaotic quantum systems, where the eigenstates are delocalized. (ii) The defect cannot be placed on the edges of the chain, because in this case the system is still integrable [35]. (iii) The defect should not be too large, because it would break the chain in two. By this we mean an excitation on one side of the chain would not have enough energy to overcome the defect and then reach the other side of the chain. In practice, we would be dealing with two independent chains described by the XXZ model, which is an integrable model [36, 37].

III. QUANTUM CHAOS

We use the level spacing distribution to identify when the system becomes chaotic. We analyze also what happens to the structure of the eigenstates once level repulsion sets in.

A. Level spacing distribution

The level spacing distribution is simply a histogram of the spacings s of neighboring energy levels [7, 8, 15]. Energy levels of integrable systems are not correlated, they are not prohibited from crossing, so the distribution is Poissonian,

$$P_P(s) = \exp(-s). \quad (4)$$

In chaotic systems, the eigenvalues become correlated and crossings are avoided; there is level repulsion and the level spacing distribution is given by the Wigner-Dyson distribution, as predicted by random matrix theory. The form of the Wigner-Dyson distribution depends on the symmetry properties of the Hamiltonian. Systems with time reversal invariance are described by Gaussian Orthogonal Ensembles (GOEs). A GOE corresponds to an ensemble of real symmetric matrices, whose elements H_{ij} are independent random numbers from a Gaussian distribution. The average of the elements and the variance satisfy $\langle H_{ij}\rangle = 0$ and $\langle H_{ij}^2\rangle = 1 + \delta_{ij}$. The level spacing distribution of a GOE is given by

$$P_{WD}(s) = (\pi s/2)\exp(-\pi s^2/4). \quad (5)$$

The Hamiltonian describing our system, H (1), is also real and symmetric, so the distribution achieved in the chaotic limit is the same $P_{WD}(s)$ above. However, as we said in the introduction, not all features of a GOE can be reproduced by a system with two-body interactions, as our own. The density of states (histogram of energy levels), for instance, is Gaussian for model (1) but semicircular for the GOE. The interested reader may obtain these two shapes with the codes provided in the supplementary material [43]. Another difference is the structure of the eigenstates, as further discussed in Sec.III.B. For GOEs, all eigenstates are similar and highly delocalized, whereas for model (1), delocalization is restricted to the middle of the spectrum.

In order to obtain the level spacing distribution, we need first to separate the eigenvalues according to their symmetry sectors (subspaces). If we mix eigenvalues from different symmetry sectors, we may not achieve a Wigner-Dyson distribution even if the system is chaotic. This is because eigenvalues from different subspaces are independent and therefore uncorrelated, so they have no reason to repel each other. We discuss further the danger of mixing eigenvalues from different symmetry sectors in Sec.IV. For the moment, we only need to remember that H (1) conserves S^z. This symmetry implies that the Hamiltonian matrix is separated into uncoupled blocks, each corresponding to a subspace with a fixed number of spins pointing up. In the studies below, we select a particular subspace with $L/3$ up-spins and thus dimension $dim = L!/[(L/3)!(L - L/3)!]$.

The second essential step before computing the histogram is to unfold the spectrum. The procedure consists of locally rescaling the energies, so that the local density of states of the renormalized eigenvalues is 1. This allows for the comparison of spectra obtained for different parameters and even for different systems. In practice, there are different ways to unfold the spectrum. A simple and commonly used recipe is the following: (i) make sure the spectrum is ordered in increasing values of energy; (ii) separate it into several smaller sets of eigenvalues; and (iii) divide each eigenvalue by the mean level spacing of its particular set. The mean level spacing of

the new set of renormalized energies becomes, of course, 1. Since the density of states is the number of states in an interval of energy, that is the reciprocal of the mean level spacing, this procedure ensures also that the local density of states is unity. This recipe is the one used in the codes available in the supplementary material [43].

In hand of the unfolded spacings of neighboring levels, the histogram can now be computed. Notice that to compare it with the theoretical curves, the distribution needs to be normalized, so that its total area is equal to 1.

Figure 1 shows the level spacing distribution for the cases where the defect is placed on site 1 (left panel) and on site $\lfloor L/2 \rfloor$ (right panel). The first corresponds to an integrable model and the distribution is Poissonian, while the second is a chaotic system, so the distribution is Wigner-Dyson.

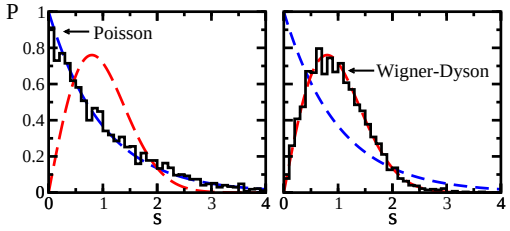

FIG. 1: (Color online.) Level spacing distribution for H (1) with $L = 15$, 5 spins up, $\omega = 0$, $\epsilon_d = 0.5$, $J_{xy} = 1$, and $J_z = 0.5$ (arbitrary unit); bin size = 0.1. Left panel: defect on site $d = 1$; right panel: defect on site $d = 7$. Dashed lines: theoretical curves.

B. Number of principal components

We now proceed to investigate how the transition from a Poisson to a Wigner-Dyson distribution affects the structure of the eigenstates. In particular, we study how much delocalized they are in both regimes.

In order to determine how much the eigenstates spread in a particular basis, we look at their components. Consider an eigenstate $|\psi_i\rangle$ written in the basis vectors $|\xi_k\rangle$ as $|\psi_i\rangle = \sum_{k=1}^{dim} c_{ik}|\xi_k\rangle$. It will be localized if it has the participation of few basis vectors, that is if few $|c_{ik}|^2$ make significant contributions. It will be delocalized if many $|c_{ik}|^2$ participate with similar values. To quantify these ideas, we use the sum of the square of the probabilities, $|c_{ik}|^4$ (the sum of the probabilities would not be a good choice, since normalization implies $\sum_{k=1}^{dim} |c_{ik}|^2 = 1$), and define the number of principal components (NPC) [27, 28] as

$$\mathrm{NPC}_i \equiv \frac{1}{\sum_{k=1}^{dim} |c_{ik}|^4}. \qquad (6)$$

NPC gives the number of basis vectors that contribute to each eigenstate. It is small when the state is localized and large when the state is delocalized.

For GOEs, the eigenstates are random vectors, *i.e.* the amplitudes c_{ik} are independent random variables. These states are completely delocalized. Complete delocalization does not mean, however, that NPC=dim. Because the weights $|c_{ik}|^2$ fluctuate, the average over the ensemble gives NPC $\sim dim/3$ [27, 28].

To study NPC for model (1), we need first to choose a basis. This choice depends on the question we want to address. We consider two bases, the site- and the mean-field basis. The site-basis is appropriate when analyzing the level of spatial delocalization of the system. To separate regular from chaotic behavior, a more appropriate basis consists of the eigenstates of the integrable limit of the model, which is referred to as the mean-field basis [27]. In our case, the integrable limit corresponds to Hamiltonian (1) with $J_{xy}, \epsilon_d \neq 0$ and $J_z = 0$.

In our numerics, we start by writing the Hamiltonian in the site-basis. Let us denote these basis vectors by $|\phi_j\rangle$. In the absence of Ising interaction, the diagonalization of the Hamiltonian leads to the mean-field basis vectors. They are given by $|\xi_k\rangle = \sum_{j=1}^{dim} b_{kj}|\phi_j\rangle$. The diagonalization of the complete matrix, including Ising interaction, gives the eigenstates in the site-basis, $|\psi_i\rangle = \sum_{j=1}^{dim} a_{ij}|\phi_j\rangle$. Using the relationship between $|\phi_j\rangle$ and $|\xi_k\rangle$, we may also write the eigenstates of the total H (1) in the mean-field basis as

$$|\psi_i\rangle = \sum_{k=1}^{dim} \left(\sum_{j=1}^{dim} a_{ij} b^*_{kj} \right) |\xi_k\rangle = \sum_{k=1}^{dim} c_{ik}|\xi_k\rangle. \qquad (7)$$

Figure 2 shows NPC for the eigenstates in both the site-basis (top panels) and the mean-field basis (bottom panels) for the cases where the defect is placed on site 1 (left panels) and on site $\lfloor L/2 \rfloor$ (right panels). The level of delocalization increases significantly in the chaotic regime (right panels). However, contrary to random matrices, the largest values are restricted to the middle of the spectrum, the states at the edges being more localized. This is a reflection of the Gaussian shape of the density of states of systems with two-body interactions. The highest concentration of states appears in the middle of the spectrum. It is there that strong mixing of states can happen leading to widely spread eigenstates.

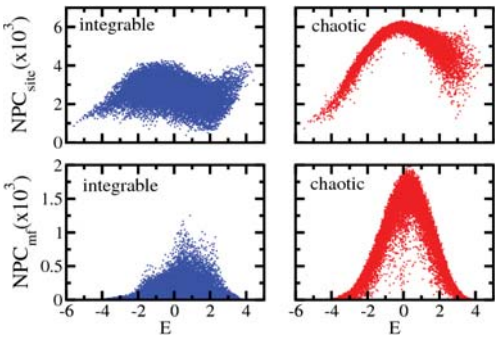

FIG. 2: (Color online.) Number of principal components for the eigenstates of H (1) vs energy; $L = 18$, 6 spins up, $\omega = 0$, $\epsilon_d = 0.5$, $J_{xy} = 1$, and $J_z = 0.5$ (arbitrary unit). Top panels: site-basis; bottom panels: mean-field basis. Left panels: defect on site $d = 1$; right panels: defect on site $d = 9$.

An interesting difference between the integrable and chaotic regimes are the fluctuations of the values of NPC. For

the regular system (left panels) NPC shows large fluctuations, whereas in the chaotic regime (right panels) NPC approaches a smooth function of energy. The onset of chaos leads to the uniformization of the eigenstates. Chaotic eigenstates close in energy have similar structures and consequently similar values of NPC.

IV. SYMMETRIES

The presence of the defect breaks symmetries of the system, which so far we did not have to worry about. In this section, we remove the defect and have a closer look at them.

We refer to the system in the absence of defect ($\epsilon_d = 0$) as clean. Contrary to the defect-case, a clean spin-1/2 chain with NN couplings remains integrable even when the Ising interaction is added. This system can be analytically solved using a method known as Bethe ansatz [36]. A pedagogical introduction to this method may be found in Ref.[37]. To drive the system to the chaotic limit, while keeping it clean, we need to add further couplings. By considering couplings between next-nearest-neighbors (NNNs) [38–41], the Hamiltonian becomes

$$H = H_{\rm NN} + \alpha H_{\rm NNN}, \tag{8}$$

where

$$H_{\rm NNN} = \sum_{n=1}^{L-2} \left[J'_{xy} \left(S^x_n S^x_{n+2} + S^y_n S^y_{n+2} \right) + J'_z S^z_n S^z_{n+2} \right] .$$

For α sufficiently large ($\alpha \gtrsim 0.2$ when $L = 15$), there are various scenarios where chaos may develop, which include: (i) absence of Ising interactions, $J_z = J'_z = 0$; (ii) absence of flip-flop term between NNNs, $J'_{xy} = 0$; (iii) absence of Ising interaction between NNNs, $J'_z = 0$, and (iv) presence of all four terms.

Depending on the parameters of H (8), however, we may not obtain a Wigner-Dyson distribution even if the system is chaotic. This happens if not all symmetries of the system are taken into account [39, 41]. We have already mentioned conservation of total spin in the z direction. In the absence of defect, other symmetries of H (8) include [42]:

• *Parity*. Parity may be understood by imagining a mirror in one edge of the chain. For eigenstates written in the site-basis, the probability of each basis vector is equal to that of its reflection. For example, suppose we have $L = 4$ and one excitation. The eigenstates are given by $|\psi_i\rangle = a_{i1}|\uparrow\downarrow\downarrow\downarrow\rangle + a_{i2}|\downarrow\uparrow\downarrow\downarrow\rangle + a_{i3}|\downarrow\downarrow\uparrow\downarrow\rangle + a_{i4}|\downarrow\downarrow\downarrow\uparrow\rangle$. The amplitudes will either be $a_{i1} = a_{i4}$ and $a_{i2} = a_{i3}$ in the case of even parity, or $a_{i1} = -a_{i4}$ and $a_{i2} = -a_{i3}$ in the case of odd parity. The level spacing distribution needs to be independently obtained for each parity sector.

• *Spin reversal*. If the chain has an even number of sites and $L/2$ up-spins, then $S^z = 0$. In this sector, pairs of equivalent basis vectors correspond to those which become equal if we rotate all the spins from one vector by 180^o. For example, state $|\uparrow\downarrow\downarrow\uparrow\rangle$ pairs with state $|\downarrow\uparrow\uparrow\downarrow\rangle$.

• *Total spin*. If the system is isotropic, *i.e.* all couplings have the same strength, $J_{xy} = J_z$ and $J'_{xy} = J'_z$, total spin, $S^2 = (\sum_{n=1}^{L} \vec{S}_n)^2$, is conserved.

Notice that in the case of closed boundary conditions, there is also momentum conservation. The more symmetries the system has, the smaller the subspaces become for a certain system size, which is not good for statistics. This explains why we chose open boundary conditions throughout this work.

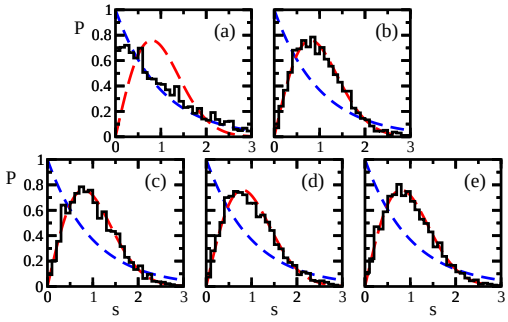

FIG. 3: (Color online.) Level spacing distribution for H (8) with $\alpha = 0.5$, $J_{xy} = 1$ (arbitrary unit); bin size = 0.1. Panel (a): $L = 14$, 7 spins up, $J'_{xy} = J_z = J'_z = 1$; all eigenvalues of the subspace $S^z = 0$ are considered. Panels (b), (c), (d) and (e): $L = 15$, 5 spins up. The eigenvalues are separated according to the parity of the corresponding eigenstates; $P(s)$ is the average of the distributions of the two parity sectors. Panel (b): $J'_{xy} = 1$, $J_z = J'_z = 0.5$. Panel (c): $J'_{xy} = 1$, $J_z = J'_z = 0$. Panel (d): $J'_{xy} = 0$, $J_z = J'_z = 0.5$. Panel (e): $J'_{xy} = 1$, $J_z = 0.5$, $J'_z = 0$.

In Fig. 3 we show the level spacing distribution for the four chaotic systems described above, (i)-(iv). All panels deal with eigenvalues of a single selected S^z-sector. In panels (b), (c), (d), and (e), we circumvent the $S^z = 0$ subspace by avoiding chains with an even number of sites. We also choose $J_z \neq J_{xy}$ to avoid conservation of total spin. In doing so, the only remaining symmetry is parity, which we do take into account. The expected Wigner-Dyson distributions are then obtained. Both panels (a) and (b) show results for a chaotic spin-1/2 chain from category (iv). Contrary to panel (b), panel (a) mixes the three symmetries itemized above, which explains why $P(s)$ becomes a misleading Poisson distribution.

V. CONCLUSION

We provided a detailed explanation of how to compute the level spacing distribution of a quantum system and used it to verify when a one-dimensional system of interacting spins-1/2 becomes chaotic. A simple recipe to unfold the spectrum and the importance of taking into account the symmetries of the system before making the histogram were discussed. We also used the number of principal components to quantify the level of delocalization of the eigenstates and to compare the results for integrable and chaotic domains. The number of principal components were computed in two different bases and an expression to change the basis in which the eigenstates

are written was given.

Spin-1/2 chains are excellent models to introduce students to basic concepts of linear algebra and quantum mechanics, from matrix diagonalization to the time evolution of the wave functions. They serve also as a starting point to explore various topics of current research in physical, biological and computer science. To motivate further studies and to facilitate the understanding of the present paper, the computer programs used to obtain the data for Figs. 1, 2, and 3 are available online in [43]. There, the reader will also find codes to study GOEs and suggestions for other exercises.

Acknowledgments

A. G. thanks Stern College for Women of Yeshiva University for a summer fellowship and the Kressel Research Scholarship for a one-year financial support. This work is part of her thesis for the S. Daniel Abraham Honors Program. L. F. S. thanks M. Edelman, F. M. Izrailev, and F. Zypman for useful discussions.

[1] H. Poincaré, *Science and Method* (Thomas Nelson and Sons, London, 1914).
[2] J. Gleick, *Chaos: Making a New Science* (Viking, New York, 1987).
[3] R. V. Jensen, "Quantum Chaos", Nature **355**, 311-318 (1992).
[4] M. Gutzwiller, "Quantum Chaos", Sci. Am., **206**, 78–84 (1992).
[5] Z. Rudnick, "Quantum Chaos?", Notices of the AMS, **55**, 32–34, (January, 2008).
[6] M. C. Gutzwiller, *Chaos in Classical and Quantum Mechanics* (Springer-Verlag, New York, 1990).
[7] F. Haake, *Quantum Signatures of Chaos* (Springer-Verlag, Berlin, 1991).
[8] L. E. Reichl, *The transition to chaos: conservative classical systems and quantum manifestations* (Springer, New York, 2004).
[9] H.-J. Stöckmann, *Quantum Chaos: An Introduction* (Cambridge University Press, Cambridge, 2007).
[10] M. V. Berry, "Quantum scars of classical closed orbits in phase space", Proc. R. Soc. Lond. A **423**, 219–231 (1989).
[11] E. J. Heller, "Bound-State Eigenfunctions of Classically Chaotic Hamiltonian Systems: Scars of Periodic Orbits", Phys. Rev. Lett. **53**, 1515–1518 (1984).
[12] S. W. McDonald and A. N. Kaufman, "Spectrum and Eigenfunctions for a Hamiltonian with Stochastic Trajectories", Phys. Rev. Lett. **42**, 1189–1191 (1979).
[13] M. V. Berry, "Quantizing a classically ergodic system: Sinai's billiard and the KKR method", Ann. Phys. (NY) **131**, 163-216 (1981).
[14] O. Bohigas, M. J. Giannoni and C. Schmit, "Characterization of Chaotic Quantum Spectra and Universality of Level Fluctuation Laws" Phys. Rev. Lett. **52**, 1–4 (1984).
[15] T. Guhr, A. Mueller-Gröeling, and H. A. Weidenmüller, "Random Matrix Theories in Quantum Physics: Common Concepts", Phys. Rep. **299**, 189–425 (1998).
[16] T. Timberlake, "Random numbers and random matrices: Quantum chaos meets number theory", Am. J. Phys. **74**, 547–553 (2006).
[17] E. P. Wigner, "On the statistical distribution of the widths and spacings of nuclear resonance levels", Proc. Cambridge Phil. Soc. **47**, 790–798 (1951).
[18] C. W. J. Beenakker, "Random-matrix theory of quantum transport", Rev. Mod. Phys. **69**, 731–808 (1997).
[19] Y. Alhassid, "The Statistical Theory of Quantum Dots", Rev. Mod. Phys. **72**, 895–968 (2000).
[20] M. V. Berry, "Regular and irregular semiclassical wavefunctions", J. Phys. A **10**, 2083 (1977).
[21] T. A. Brody, J. Flores, J. B. French, P. A. Mello, A. Pandey, and S. S. M. Wong, Rev. Mod. Phys **53**, 385 (1981).
[22] E. P. Wigner, "Characteristic Vectors of Bordered Matrices with Infinite Dimension", Ann. Phys. **62**, 548–564 (1955).
[23] J. B. French and S. S. M. Wong, Phys. Lett. B **33**, 449–452 (1970).
[24] O. Bohigas and J. Flores, Phys. Lett. B **34**, 261–263 (1971).
[25] J. Flores, M. Horoi, M. Müller, and T. H. Seligman, Phys. Rev. E **63**, 026204 (2001).
[26] V. K. B. Kota, "Embedded random matrix ensembles for complexity and chaos in finite interacting particle systems ", Phys. Rep. **347**, 223–288 (2001).
[27] V. Zelevinsky, B. A. Brown, N. Frazier, and M. Horoi, "The Nuclear Shell Model as a Testing Ground For Many-Body Quantum Chaos", Phys. Rep. **276**, 85–174 (1996).
[28] F. M. Izrailev, "Simple–Models Of Quantum Chaos – Spectrum And Eigenfunctions", Phys. Rep. **196**, 299–392 (1990).
[29] G. Casati, B. V. Chirikov, I. Guarneri, and F. M. Izrailev, "Band-random-matrix model for quantum localization in conservative systems", Phys. Rev. E **48**, R1613–R1616 (1993).
[30] V. V. Flambaum, A. A. Gribakina, G. F. Gribakin, and M. G. Kozlov, "Structure of compound states in the chaotic spectrum of the Ce atom: localization properties, matrix elements, and enhancement of weak perturbations", Phys. Rev. A **50**, 267–296 (1994).
[31] S. Trotzky, P. Cheinet, S. Fölling, M. Feld, U. Schnorrberger, A. M. Rey, A. Polkovnikov, E. A. Demler, M. D. Lukin, and I. Bloch, "Time–resolved observation and control of superexchange interactions with ultracold atoms in optical lattices," *Science*, vol. 319, pp. 295–299, 2008.
[32] J. Simon, W. S. Bakr, R. Ma, M. E. Tai, P. M. Preiss, and M. Greiner, "Quantum Simulation of Antiferromagnetic Spin Chains in an Optical Lattice", Nature **472**, 307–312 (2011).
[33] Y.-A. Chen, S. Nascimbène, M. Aidelsburger, M. Atala, S. Trotzky, and I. Bloch, "Controlling correlated tunneling and superexchange interactions with ac-driven optical lattices." arXiv:1104.1833.
[34] L. F. Santos, "Integrability of a disordered Heisenberg spin-1/2 chain", J. Phys. A **37**, 4723–4729 (2004).
[35] F. C. Alcaraz, M. N. Barber, M. T. Batchelor, R. J. Baxter, and G. R. W. Quispel, "Surface Exponents of the Quantum XXZ, Ashkin-Teller And Potts Models", J. Phys. A **20**, 6397–6409 (1987).
[36] H. A. Bethe, "On the Theory of Metal I. Eigenvalues and Eigenfunctions of a Linear Chain of Atoms", Z. Phys. **71**, 205–217 (1931).
[37] M. Karbach and G. Müller, "Introduction to the Bethe ansatz I", Comput. Phys. **11**, 36–44 (1997); arXiv:cond-mat/9809162.
[38] T. C. Hsu and J. C. Angles d'Auriac, "Level Repulsion In In-

tegrable And Almost-Integrable Quantum Spin Models", Phys. Rev. B **47**, 14291–14296 (1993).

[39] K. Kudo and T. Deguchi, "Level Statistics of XXZ Spin Chains with Discrete Symmetries: Analysis through Finite-size Effects ", J. Phys. Soc. Jpn. **74**, 1992–2000 (2005).

[40] L. F. Santos and M. Rigol, "Onset of quantum chaos in one-dimensional bosonic and fermionic systems and its relation to thermalization", Phys. Rev. E **81**, 036206 (2010).

[41] L. F. Santos, "Transport and control in one-dimensional systems", J. Math. Phys. **50**, 095211 (2009).

[42] W. G. Brown, L. F. Santos, D. J. Starling, and L. Viola, "Quantum Chaos, Localization, and Entanglement in Disordered Heisenberg Models", Phys. Rev. E **77**, 021106 (2008).

[43] Supplementary material at http://www.yu.edu/faculty/santos/.